



Decoding the byssus fabrication by spatiotemporal secretome analysis of scallop foot



Xiaoting Dai^{a,1}, Xuan Zhu^{a,1}, Lisui Bao^{c,1}, Xiaomei Chen^a, Yan Miao^a, Yangping Li^a, Yuli Li^{a,b}, Jia Lv^a, Lingling Zhang^a, Xiaoting Huang^{a,d}, Zhenmin Bao^{a,d,e}, Shi Wang^{a,b,e,*}, Jing Wang^{a,b,*}

^aSars-Fang Centre & MOE Key Laboratory of Marine Genetics and Breeding, College of Marine Life Sciences, Ocean University of China, Qingdao 266003, China

^bLaboratory for Marine Biology and Biotechnology, Qingdao National Laboratory for Marine Science and Technology, Qingdao 266237, China

^cInstitute of Evolution & Marine Biodiversity, Ocean University of China, Qingdao 266003, China

^dLaboratory for Marine Fisheries Science and Food Production Processes, Qingdao National Laboratory for Marine Science and Technology, Qingdao 266237, China

^eLaboratory of Tropical Marine Germplasm Resources and Breeding Engineering, Sanya Oceanographic Institution, Ocean University of China, Sanya 572000, China

ARTICLE INFO

Article history:

Received 5 April 2022

Received in revised form 24 May 2022

Accepted 24 May 2022

Available online 27 May 2022

Keywords:

Byssal secretome

Bioadhesion

Scallop

Foot

Spatiotemporal transcriptomes

ABSTRACT

Secretome is involved in almost all physiological, developmental, and pathological processes, but to date there is still a lack of highly-efficient research strategy to comprehensively study the secretome of invertebrates. Adhesive secretion is a ubiquitous and essential physiological process in aquatic invertebrates with complicated protein components and unresolved adhesion mechanisms, making it a good subject for secretome profiling studies. Here we proposed a computational pipeline for systematic profiling of byssal secretome based on spatiotemporal transcriptomes of scallop. A total of 186 byssus-related proteins (BRPs) were identified, which represented the first characterized secretome of scallop byssal adhesion. Scallop byssal secretome covered almost all of the known structural elements and functional domains of aquatic adhesives, which suggested this secretome-profiling strategy had both high efficiency and accuracy. We revealed the main components of scallop byssus (including EGF-like domain containing proteins, the Tyr-rich proteins and 4C-repeats containing proteins) and the related modification enzymes primarily contributing to the rapid byssus assembly and adhesion. Spatiotemporal expression and co-expression network analyses of BRPs suggested a simultaneous secretion pattern of scallop byssal proteins across the entire region of foot and revealed their diverse functions on byssus secretion. In contrast to the previously proposed “root-initiated secretion and extension-based assembly” model, our findings supported a novel “foot-wide simultaneous secretion and in situ assembly” model of scallop byssus secretion and adhesion. Systematic analysis of scallop byssal secretome provides important clues for understanding the aquatic adhesive secretion process, as well as a common framework for studying the secretome of non-model invertebrates.

© 2022 The Author(s). Published by Elsevier B.V. on behalf of Research Network of Computational and Structural Biotechnology. This is an open access article under the CC BY-NC-ND license (<http://creativecommons.org/licenses/by-nc-nd/4.0/>).

1. Introduction

Secretory proteins include many enzymes, toxins, and antimicrobial peptides, which are involved in almost all physiological, developmental, and pathological processes. The discoveries and applications of potential secretory proteins in regenerative medicine, cancer diagnosis and therapy are pioneering and have spawned the area of secretomics [1–4]. In recent years, secretomic studies have expanded throughout life science, from human dis-

eases to bioadhesion, biomineralization, and mucous secretion processes in various organisms. Bioadhesives, particularly secreted by aquatic invertebrates, have long intrigued researchers since their unique “water-resistant glue” like properties and biocompatible characteristics are convenient for developing biomedical materials (e.g., surgical adhesives) [5–7]. In addition, adhesive secretion is a ubiquitous and essential physiological process in aquatic invertebrates (> 5,000 species), which help animals steadily attach to different substrates and facilitate diverse physiological processes including larval metamorphosis, reproduction, prey capture and intertidal zone fixation [8–10]. Thus it is suggested that bioadhesion promotes adaptive radiations of species in violently fluctuant environments [9,11–14].

* Corresponding authors.

E-mail addresses: swang@ouc.edu.cn (S. Wang), wangjing8200@ouc.edu.cn (J. Wang).

¹ These authors contributed equally to this work.

As a large animal group of phylum Mollusca, scallops are well-known for their effective adhesion ability to adapt to turbulent currents, who can attach to substrates for metamorphosis at pediveliger larvae stage by strong byssal threads which are retained in adults for semi-sessile life [15]. It has been demonstrated that foot is the adhesive organ of scallop as many byssal glands were located in different foot regions [16]. Unlike the permanent adhesion of sessile bivalves (e.g., mussels), scallop remains the ability to discard its byssus instantly under certain adverse conditions, and to reattach to new substrates by rapid secretion of new byssus, which has been proposed as a key biological characteristic for its successful adaptation to various habitats [12,17]. Moreover, according to our previous study on Zhikong scallop *Chlamys farreri* (Jones et Preston, 1904) [17,18], scallops can secrete more abundant byssus than mussels and possess distinct protein composition and unusual assembly mechanisms [17,19–21]. The unique adhesive characteristics of scallop byssus make it a valuable biological model to study the dynamic adhesive secretomic process of byssal detachment and reattachment. However, the molecular mechanism behind still remains elusive.

Due to the complicated nature of secretory pathways, the studies of the adhesive secretome in aquatic species are lagging behind. It has been demonstrated that aquatic adhesive proteins share very low sequence similarity across species [22,23] and adhesive mechanisms are diverse among different aquatic organisms [24,25]. Currently, the adhesive proteins have only been identified from few aquatic species by two major approaches [26]. The mass spectrometry (MS)-based proteomics is regarded as the gold standard with high sensitivity to detect trace secretory proteins, while the procedure is time-consuming and requires prior proteome annotation [5]. In contrast, RNA-seq could be used for *de novo* high-throughput secretome identification, but the false-positive rate is high and subsequent functional validation is needed [27,28]. Moreover, adhesive secretion is a time-dependent complex process, but the traditional “one-time snapshot” way of secretome identification ignores the dynamic regulatory information. Due to the technique limitations mentioned above, only 16 candidate byssus-related proteins (BRPs) of scallop have been identified to date by mass spectrometric analysis [17], with systematic protein components of scallop byssus unreported and the regulatory mechanisms of byssal secretion and attachment elusive.

Here we reported a systematic computational pipeline based on both sequence feature extraction and spatiotemporal expression analysis for the construction of scallop byssal secretome. The byssal secretome refers to a set of BRPs secreted by the foot of scallop that participate in the secretion and assembly process of byssus. Our findings revealed novel byssal secretory mechanisms that may underlie scallop’s adaptation to semi-sessile life. The findings would not only shed light on the understanding of the aquatic adhesive secretion process, but also provide valuable molecular resources for further exploration of adhesive biomaterial. The proposed strategy represents an effective framework for future secretome analysis of non-model invertebrates.

2. Methods

2.1. Data source and preprocessing

A large-scale RNA sequencing dataset derived from adult tissues/organs, major developmental stages and spatiotemporal transcriptome data of foot were obtained from the *C. farreri* genome project (Table S1) [17]. The spatiotemporal transcriptomes data covered three different foot regions (proximal end, middle region and distal end, as shown in Fig. 1a) and five time points during byssal secretion (t0–4, as shown in Fig. 1b) were also included.

The old byssal threads dropped off from foot at 1 h (t1) after cutting off the byssus fibers (t0), and then, the scallop foot stucked out of the shell for environmental perception and began to secrete byssus for a new attachment after another 30 mins (t2). At 12 h, the new byssus in white color started to attach to the substrate (t3). Finally, the byssus established a stable adhesion with the substrate at 24 h (t4). The reference genome of *C. farreri* was downloaded from an open-access genomics platform for Mollusca [29] (MolluscDB, <https://mgbase.qnlm.ac>). High quality reads (> 80% base calls a quality value > 20) were retained using software fqtrim v.0.9.7, and then were mapped to the reference genome of *C. farreri* using STAR (version 2.7.1c) with default parameters [30]. Mapped reads assigned to the exon regions were counted using featureCounts (v1.6.5) and TPM (Transcripts Per Kilobase of exon model per Million mapped reads) value was calculated to represent the expression level of each gene [31]. The principal component analysis (PCA) was performed with the top 5000 most variable genes among the five time points using the factoextra R package [32].

2.2. Construction of scallop byssal secretome

We searched all the reported marine adhesive proteins identified from the bioadhesives of eight representative marine adhesive organisms from published papers [17,19,20,33–44]. According to the accession ID provided in these papers, we downloaded the protein sequences from NCBI or UNIPROT [45,46] with no more inclusion or exclusion criteria. For some proteins without the accession ID, we got the amino acid sequences from the source papers. Finally, 144 adhesive proteins (Table S2) identified from the bioadhesives were obtained and constituted a gene set of “known marine adhesive proteins” used for the follow-up analysis. As an inherent N-terminal sequence of classic secretory proteins, signal peptides of reported adhesive proteins were predicted using SignalP [47]. More than 85% of the marine adhesive proteins (Fig. 1c) were signal peptide positive, which suggested the reasonability of screening scallop adhesive proteins by signal peptide. Thus, we developed a computational pipeline according to the classical protein secretion pathway [48] to systematically identify the foot secreted proteins closely linked to byssus fabrication, which form the byssal secretome of *C. farreri* (Fig. 1).

The first two steps screened the up-regulated and highly expressed genes during byssus secretion, aiming to eliminate redundant proteins in byssal secretome. Firstly, based on the spatiotemporal transcriptomes (three regions across the foot: proximal end, middle region and distal end, Fig. 1a; at five time points: t0–4, Fig. 1b), the up-regulated genes (up-DEGs) at t1–4 time points against t0 were obtained using the R package RNNentropy [49], with the criteria of the corrected global sample specificity test $P < 0.01$ by the Benjamini–Hochberg method and the local sample specificity test $P < 0.01$. Then up-DEGs with TPM > 50 (average expression level of all genes) in at least one foot region were selected, following with the signal peptide prediction using SignalP [47] and only signal peptide positive proteins were kept. To exclude membrane proteins, transmembrane segments of signal peptide positive proteins were screened using THMHMM v2.0 webserver [50] and MCMBB webserver [51]. Then proteins without alpha-helix (i.e., 'PredHel = 0' or 'PredHel = 1 and First60 > 10') and beta-sheet (MCMBB score < 0) were further screened by TargetP v2.0 [52] to exclude cytosolic proteins. Finally, the retained proteins were identified as byssus related proteins (BRPs) and used in following analysis.

2.3. Sequence characteristics and expression patterns of identified BRPs

According to the genome annotation file of *C. farreri*, the gene structures (gene length, number of exon and ORF length) of 186

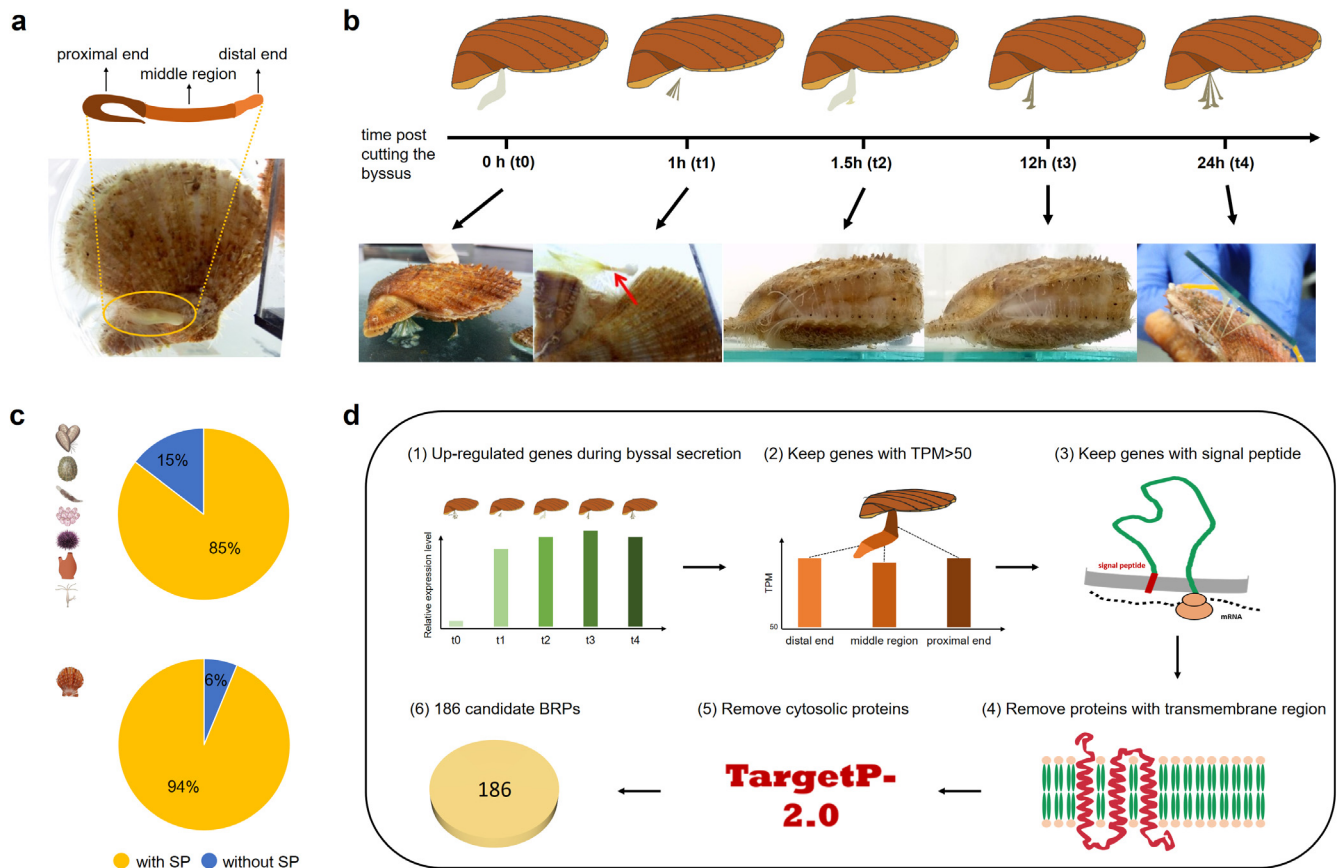


Fig. 1. Profiling of byssal secretome based on spatiotemporal transcriptomes of scallop. (a) Photographs of *C. farreri* and the diagram showing different regions of the foot. (b) The byssus secretion process across 5 time points (t0–4). The old byssal threads dropped out from foot at 1 h (t1) after cutting off the byssus fibers (t0), and then, the scallop foot stuck out of the shell for environmental perception and began to secrete byssus for a new attachment after another 30 min (t2). At 12 h, the new byssus was observed in white and attached to the substrate (t3). Finally, the byssus established a stable adhesion with the substrate at 24 h (t4). Red arrows indicated the byssus. (c) The pie charts showing that 85% of the adhesive proteins from 144 reported marine adhesives (top) and 94% of the 16 adhesive proteins identified from byssus of *C. farreri* (bottom) were signal peptide positive proteins. (d) The computational pipeline to identify the scallop byssal secretome. Based on the spatiotemporal transcriptomes, the up-regulated genes (up-DEGs) at t1–4 time points against t0 with expression level TPM > 50 were obtained firstly, following with screening of signal peptide. Then signal peptide-positive proteins were checked for transmembrane segment, only proteins without transmembrane segment were further screened by TargetP v2.0 to exclude cytosolic proteins. Finally, the retained proteins were identified as byssus related proteins (BRPs) and used in following analysis. (For interpretation of the references to color in this figure legend, the reader is referred to the web version of this article.)

identified BRPs were obtained and summarized in Table S3. Amino acid composition of BRPs was calculated using a self-written Perl script. The mass weight of BRPs were predicted using the Sequence Manipulation Suite [53]. The grand average of hydropathicities (GRAVY) of the BRPs sequence was calculated by summation of the hydropathy values of each amino acid residue, and divided by the length of the protein sequence to represent the hydropathicity of BRPs [54]. The conserved domains of scallop BRPs (Table S3) and published adhesive proteins (Table S2) obtained from the bioadhesives of seven other metazoan taxa, including four permanent adhesive species (mussel, limpet, barnacle and ciona) and three temporary adhesive species (sea urchin, hydra and flatworm) were predicted by the Batch CD-Search tool in NCBI database [55]. Though some protein sequences of ciona are not available, the domain characteristics of which were obtained from the references [37,56]. The orthologous genes were identified by comparing against the known marine adhesive proteins using BLASTP with the E-value cutoff of $1e-4$. Multiple sequence alignments of functional domain were performed using MEGA6 [57] and the alignment results were displayed by ESPript [58]. The presence of post-transcriptional modifications (PTMs) was predicted using a deep-learning framework MusiteDeep [59]. Gene ages (ps level) were estimated by using the phylostratigraphic approach as previously described by Wang et al [60]. Spatiotemporal expression pat-

terns of BRPs were shown in heatmaps. Comparison of sequence characteristics and expression patterns between 16 byssus-related proteins of scallop identified by MS and 186 BRPs identified in this study were also performed.

2.4. Gene co-expression network analysis of BRPs

A total of 15,257 up-DEGs with the TPM value higher than 5 were used for weighted gene co-expression network analysis (WGCNA) [61] with the parameters of 'softPower = 17, minModuleSize = 250 and cuttHeight = 0.99'. Different gene modules were labelled with different colors corresponding to the branch cut-off of the gene tree and unassigned genes were labeled in grey. The intramodular connectivity (K_{within}) value was used to measure the hubness of a gene in a given module, which represents the connection strength of a gene to others in the specified module [61]. To identify BRPs-related modules, over-representation analysis of 186 BRPs was performed for each module using a hypergeometric test, with P values adjusted by the Benjamini–Hochberg method for multiple-test correction [62]. GO and KEGG enrichment analysis of genes in BRPs-related modules were carried out to determine significant functions using EnrichPipeline [63]. The software Cytoscape [64] was used for co-expression network visualization.

3. Results

3.1. Construction of scallop byssal secretome

The byssal proteins of scallop are secreted by the byssus glands inside the foot and assembled outside the body. Hindered by the lack of effective profiling strategy, the secretion process, composition of byssal secretome and underlying adhesion mechanisms of scallop byssal secretion are still unclear. Traditional strategies have either as time-consuming or low throughput as MS-based proteomics or high false positive rate as RNA-seq based secretomics [5,27,28]. What's more, adhesive secretion is a time-dependent complex process, but the traditional “one-time snapshot” ways of secretome identification are usually unable to profile the dynamic regulatory process of adhesion. To overcome these limitations, we developed a systematic computational pipeline to profile the foot secretome of *C. farreri* based on the spatiotemporal transcriptomes during byssal secretion (Fig. 1a, 1b). According to the classical protein secretion pathway, secretory proteins should be characterized by N-terminal signal peptide. To verify this, we collected the amino acid sequences of 144 known marine adhesive proteins identified from adhesives in eight different taxa (Table S2). According to SignalP prediction, 85% of them possess signal peptides (Fig. 1c, top, Table S2), while the proportion was even higher (94%) in reported scallop adhesives (Fig. 1c, bottom). Thus, we incorporated this sequence characteristic into our computational pipeline to identify the scallop byssal secretome as shown in Fig. 1d. First, to avoid the “long list of candidates” obtained from comparative transcriptome analysis between adhesive organ and non-adhesive organs, we firstly screened the significantly up-regulated genes during byssus secretion, ensuring the targeted proteins were closely involved in byssal secretion and adhesion. Considering the abundant secretion of byssus, the expression levels of up-DGEs were filtered with TPM higher than the average expression level of all genes. Secreted proteins were picked out according to their signal peptide prediction. However, some proteins with signal peptides were membrane proteins or had specific retention signals that hold them back in the endoplasmic reticulum/Golgi/lysosomes [48,52]. Hence, the transmembrane proteins or cytosolic proteins were predicted and removed. Finally, the retained proteins were identified as byssus related proteins (BRPs) forming the secretome and used in following analysis.

By using this strategy, we firstly identified 1,543 up-regulated differentially expressed genes (DEGs) with expression level filtering (TPM > 50) during scallop byssal secretion. After removing potential transmembrane or cytosolic proteins, a total of 186 BRPs with signal peptide were eventually remained and regarded as the byssal secretome (Table S3), which covered 87.5% of the reported adhesive proteins in *C. farreri* detected by mass spectrometry (Fig. S1a) [17,19,21,65]. The two exceptional adhesive proteins either had low expression level (CF54475.1, average TPM = 6.82) or none predicted signal peptide (CF23353.17). The 186 BRPs were further categorized into three groups (group 1, structural BRPs; group 2, enzymes; group 3, protease inhibitors and others that could not be easily classified) according to the sequence features and functional annotations (Fig. S1b, Table S3). The gene length, ORF length, exon numbers and mass weight of identified BRPs were highly variable (see Table S3 for detail). More than 87% (162/186) BRPs were hydrophilic with GRAVY value < 0 (Fig. S1c, Table S3). Our study constructed the first secretome of scallop foot during byssal adhesion and the physicochemical properties of identified BRPs were systematically studied.

3.2. Functional domain of identified BRPs

Compared against all organisms with reported adhesive proteins (including mussel, limpet, barnacle, ciona, sea urchin, hydra

and flatworm), scallop was the only one that maintained all the total eight conserved domains (shared by > 3 metazoan taxa) in the BRPs (Fig. 2a; Table S3). In the 16 byssus-related proteins of scallop identified by MS, the EGF-like and A2M domain were found while many other domains (collagen and vWFA et al.) were absent (Fig. S2a). Among them, the EGF-like domain was most conserved as shared by seven metazoan taxa. A total of 12 BRPs containing 1 to 49 EGF-like domains were identified in the scallop byssal secretome (Fig. 2b; Table S3). 11 of those BRPs had the “EC protein” chimeric structures with 1–5 Calx-beta (CBD) domains inserted into tandem EGF-like domains (Fig. 2b; Table S3). Each EGF-like domain contained six highly conserved cysteine residues (Fig. 2b), which could form three disulfide bridges that enhanced calcium binding [66]. The longest “EC protein” CF52787.5 (i.e. Sbp9) was identified as one of the most important components of byssal root based on the proteomics approach in our earlier research. The EGFL₄ rescue assay demonstrated that the CF52787.5 protein was indispensable for byssal root integrity [19]. Among scallop BRPs, five genes contained von Willebrand factor type A (vWFA) domain with conserved DxSxS motif and TDG motif (Fig. S3a; Fig. S3b). Three collagens with 4–8 collagen domains in scallop (Fig. S3c) shared the typical triple-helical repeat (glycine-X-Y)_n with mussel byssal proteins (preCol-NG, preCol-D and preCol-P) (Fig. S3d). A scallop BRP (CF55753.4) contained EGF domain, vWFA domain, vWD domain and TSP1 domain, which was annotated as a putative adhesin (Fig. S4a). In addition, 15 other BRPs with adhesion-relevant protein domains such as LDLa, Efh, A2M and CLECT domains were also annotated as putative adhesive proteins (Fig. S4b; Table S3). Besides, a variety of enzymes (e.g., peroxidase, tyrosinase, isomerase and laccase) and protease inhibitors (e.g., metalloproteinase inhibitor, peptidase inhibitor and serine protease inhibitor) were identified as BRPs based on their functional domains (Table S3). The function of some of these BRPs have been reported in our previous studies. For instance, we proved the tyrosinase activity in foot by a catechol oxidase activity assay and the presence of DOPA in byssus threads by nitroblue tetrazolium staining, emphasizing the importance of tyrosinase in scallop byssal adhesion [17]. Biochemical analyses and protein polymerization assays implied the potential cross-linker role of the most abundant metalloproteinase inhibitor (CF9441.24, e.g. Sbp8-1, Table S5) [20]. Furthermore, another 104 BRPs were classified into group 3, 28.7% of which were molluscan specific genes (ps level ≥ 9, Table S3). In this class of BRPs, the most significant up-regulated gene was a *Bivalvia*-specific gene riched in cysteine and proline residues (CF44339.34) with function unknown (Table S3 & S4 & S4), which deserved in-depth analysis for more understanding on the evolution of scallop bioadhesives and the exploration of water-resistant adhesive biomaterial.

3.3. Amino acid composition and post-transcriptional modifications of BRPs

Biased amino acid composition and post-transcriptional modifications (PTMs) are also typical characteristics reported in bioadhesives. The BRPs had a strong preference for cysteine across all genes in *C. farreri* genome (Fig. S5a; Table S3 & S4). Principal component analysis (PCA) based on the amino acid composition revealed the sequence diversity of structural BRPs in scallop was mostly driven by glycine and proline (Fig. S5b; Table S3). Among all structural BRPs, five Cys-rich BRPs (cysteine ratio > 8%) contained multiple 4C-repeats (Fig. 2c; Table S3). Three BRPs contained significantly higher tyrosine content (Table S3, tyrosine ratio > 7%, two times higher than the mean value), one of which contained 12 repeats and shared high sequence similarity with mussel adhesive protein Mefp1 (Fig. S5c; Tables S3 & S4). Similar to the reported bioadhesives, phosphorylation, hydroxylation and glycosylation were

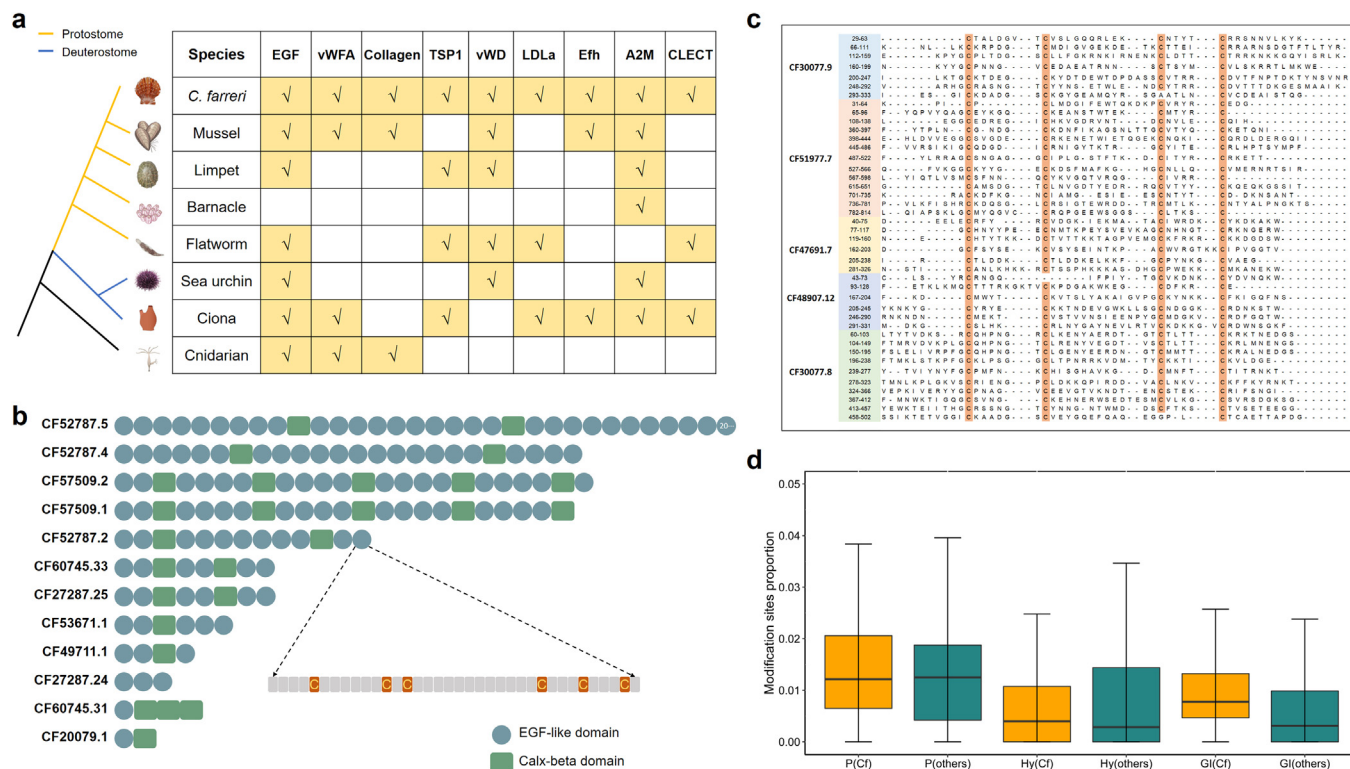


Fig. 2. Sequence characterization of scallop BRPs. (a) Commonly used domains of adhesive proteins from *C. farreri* and other seven bioadhesive taxa. (b) Exhibit of EGF-like domain containing BRPs. Eleven of them had the “EC protein” chimeric structures with 1–5 Calx-beta (CBD) domains inserted into tandem EGF-like domains. Each EGF-like domain possesses 6 conserved cysteine residues. (c) Protein sequence alignment of the 4C-repeats containing BRPs. (d) The PTM sites prediction of scallop BRPs and 144 reported adhesive proteins with the PTM scores > 0.5 (see Table S6 for details). EGF, epidermal growth factor domain; vWFA, von Willebrand factor type A-like domain; TSP1, thrombospondin 1-like domain; vWD, von Willebrand factor type D-like domain; LDLa, Low Density Lipoprotein Receptor Class A domain; Efh, EF-hand motif; A2M: Alpha-2-macroglobulin domain; CLECT: C-type lectin (CTL)/C-type lectin-like (CTLD) domain.

found as the dominant PTMs in scallop (Fig. 2d; Table S6). The latter two showed higher levels in scallop BRPs compared to other bioadhesives (Fig. 2d). Hydroxylation was mainly found on proline and lysine residues of scallop collagen and the phosphorylation was found in the Tyr-rich BRPs. Among which, CF57509.5 and CF20079.1 possessed small molecular weights (20.54/28.85 kDa) (Table S3). O-linked glycosylation and serine phosphorylation were found in a vWFA-containing BRP (CF61295.40), which was rich in six low complexity regions and two internal repeat regions (Fig. S5d; Tables S3 & S6).

3.4. Spatiotemporal transcriptome profiling of BRPs

Here, we constructed a spatiotemporal transcriptome landscape covering major developmental stages, adult tissues/organs and different foot regions (Table S1). Scallop BRPs showed significant expression bias in the adult foot (Fig. S6; Fig. S2). Consistent with the metamorphosis timing, most BRPs significantly expressed at the pedi-veliger larval stage (Fig. 3a; Fig. S2). During the secretion of scallop byssus (from t0 to t4; Fig. 1b), 186 BRPs displayed an interesting temporal expression pattern, with 66.6–74.0% of which were instantly up-regulated since the old byssal root was discharged (t1) and remained comparably high expression level until the new byssus reattached (t4) (Fig. S7; Fig. S2d). The rapid transcriptional response of BRPs to byssal secretion process was also confirmed by PCA analysis (Fig. S7).

By contrast, BRPs revealed distinct region-biased expression patterns (Fig. 3b). According to the sequence characteristics and functional annotations, 38 putative structural BRPs were further categorized into 10 groups (Fig. 3c). Collagens, vWFA domain containing proteins, 4C-repeats containing proteins and three biomin-

eralization related genes [67,68] were significantly up-regulated in the proximal end of the foot. The Tyr-rich proteins were up-regulated in the middle region and the distal end of the foot, while the amyloid, adhesin, galectin, LDLa domain containing proteins and other three biomineralization related proteins were up-regulated in the distal end of the foot [69]. The EGF-like domain containing BRPs showed an interesting expression tendency: BRPs with more EGF-like domain repeats tended to express in the proximal end whereas BRPs with less EGF domain repeats prefer expressing in the distal end (Fig. 3c), which were also observed in our previous study particularly focusing on “EC proteins” [19]. Among them, the EGF-like domain containing proteins, the Tyr-rich proteins and the 4C-repeats containing proteins displayed significantly higher expression levels than others, suggesting that they are the main components of scallop byssus (Fig. 3c). However, the expression patterns of most enzymes among BRPs were regional-uniform (Fig. S8). Phenoloxidases and peroxidases were most important modification enzymes in addition to protein processing-related BRPs. Among them, tyrosinases and peroxidase showed spatio-preferred expression patterns in different foot regions. Besides, enzymes involving in forming and breaking of disulfide bonds (*Pdia 3/5/6* and *Txndc12*) were mainly expressed in the distal end and the middle region of the foot.

3.5. Gene co-expression network of byssus secretion

The key genes and pathways involved in byssus secretory regulation of *C. farreri* were identified by constructing the weighted gene co-expression network of DEGs during byssal secretion. A total of 15,256 genes were assigned to seven modules (M1-M7) with differential expression patterns among three different foot

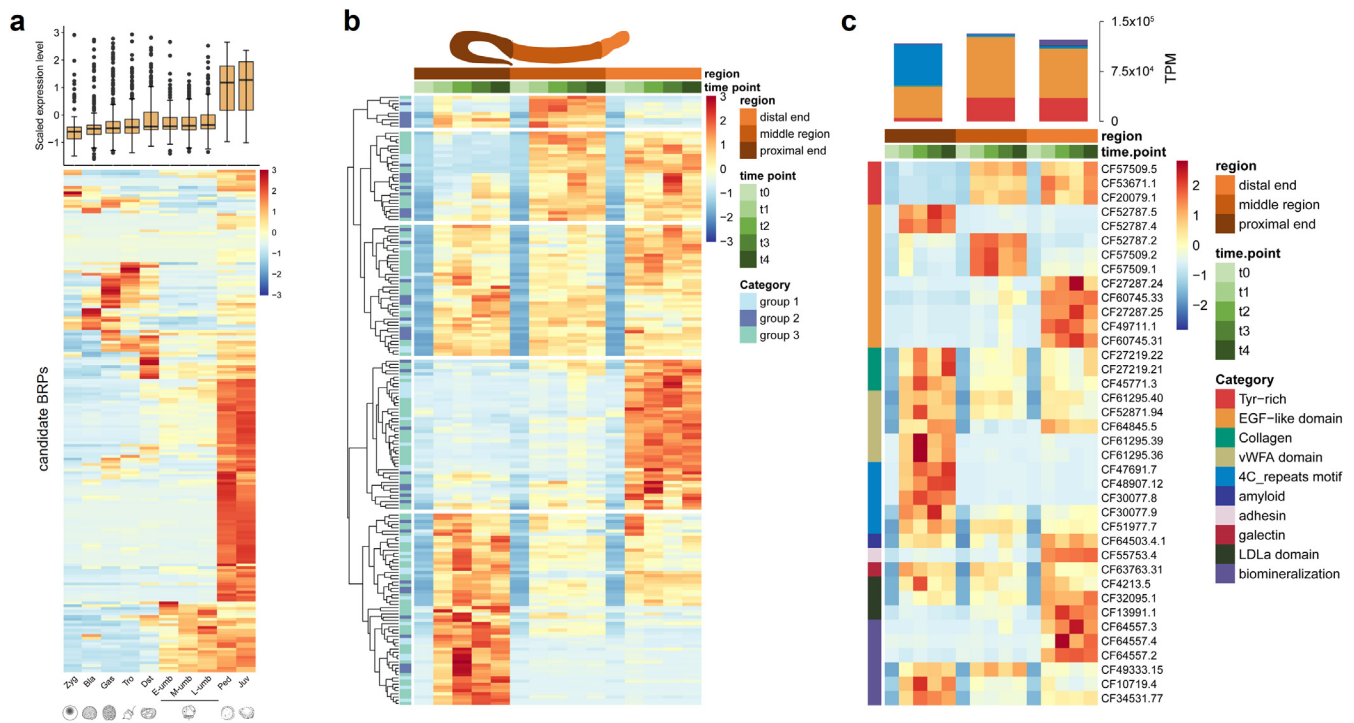


Fig. 3. Overview of the expression profile of 186 candidate BRPs. (a) The expression pattern of BRPs across developmental stages. BRPs were significantly up-regulated at the pedi-veliger larval stage and juvenile stage (one-sided paired *t*-test, *p*-value < 2.2e-16). The full description corresponding to the abbreviations of developmental stages are shown in Table S1. (b) Spatiotemporal expression of 186 candidate BRPs assigned into 3 groups, group 1–3. (c) Expression patterns of BRPs in group 1 during byssus secretion. BRPs in group 1 were assigned into 10 categories according to the characteristic of sequence. The expression levels of each category in three regions were displayed with cumulative histogram on the top panel.

regions (proximal end, middle region and distal end) and five time points (t0–4) (Fig. S9). The 186 identified BRPs were significantly enriched in three modules (M4, M5 and M7, with adjusted *p*-value < 0.01), which were thus labeled as the BRP-related modules (Fig. 4a; Table S7). The module M7 was significantly up-regulated in the proximal end. The genes in M7 were enriched in the GO terms of transmembrane transporter activity and disulfide isomerase/oxidoreductase activity related molecular functions and the KEGG pathways of O-Glycan biosynthesis signal transduction and O-Glycan biosynthesis (Fig. 4b; Tables S8 & S9). Module M5 mainly responded in the distal end, with genes participating in neurotransmitter transporter activity, metal ion binding (e.g., ferric iron binding and calcium ion binding), peroxidase activity and tyrosine metabolism (Fig. 4b; Tables S8 & S9). Compared with the other two modules, M4 genes functioned primarily in the proximal end and the middle region, which mainly involved in translation, protein processing, protein transport, disulfide bonds formation/hydrolyzation related molecular functions and cutin biosynthesis (Fig. 4b; Tables S8 & S9). A total of 15 TFs were identified as the hub genes (the top 200 genes of each module sorted by the K_{within} values) in the co-expression network of byssus secretion, suggesting their key roles in adhesive regulation (Table S10; Fig. 4c). According to the predicted functions and expression patterns of scallop BRPs, we proposed a hypothetical model of scallop byssus secretion and adhesion (Fig. 5).

4. Discussion

Originating from the “signal hypothesis” [48], signal peptide is known as the “zip code”, which is an universal sequence feature of all secretory proteins via classical pathway [52]. Indeed, we collected 144 known adhesive proteins from eight taxa, and found

that 85% of which are signal peptide-positive, suggesting the feasibility to screen adhesive proteins by integrating the sequence features. Hence, we proposed a computational pipeline to profile secretome by considering both gene composition and expression level at the same time. Using this systematic strategy, a total of 186 BRPs were identified, which represented the first secretome of scallop byssal adhesion. The identified BRPs covered almost all of the basic recipe that were summarized by Liu et al. from known aquatic adhesive proteins, including structural elements (e.g., Cys-rich domains, Tyr-rich repeats, PTMs), functional domains (e.g., EGF-like, vWFA, TSP-1, vWD), enzymes (e.g., tyrosinase, peroxidase, isomerase), proteinase inhibitors (e.g., metalloproteinase inhibitor, peptidase inhibitor and serine protease inhibitor) and others including Cys-rich and Pro-rich proteins et al. [56,70]. The most complete domain recipe was found in scallop compared against all organisms with reported adhesive proteins. It's quite possible that the reported secretomes from other species are incomplete due to the complexity of the marine adhesive proteins and the limitation of screening strategy [5,27,28]. For example, domains including collagen, vWFA, LDLa and so on were absent in the 16 MS-identified BRPs of scallop. Based on the above all, this sequencing-driven strategy proposed in this study had both high efficiency and accuracy, which provided a generic framework for other secretome profiling studies. The core gene sets obtained in this study present important resources for better understanding of marine bioadhesive systems and biomaterial design.

As an ancestral feature, bioadhesion is essential for the sessile life of scallop *C. farreri* through byssal secretion [15]. However, the secretion process, composition of byssal secretome and adhesion mechanisms during scallop byssus secretion were still unclear. Our systematic strategy for identification of scallop byssal secretome and spatiotemporal co-expression network analysis enabled us to acquire the global view of byssal secretion and illus-

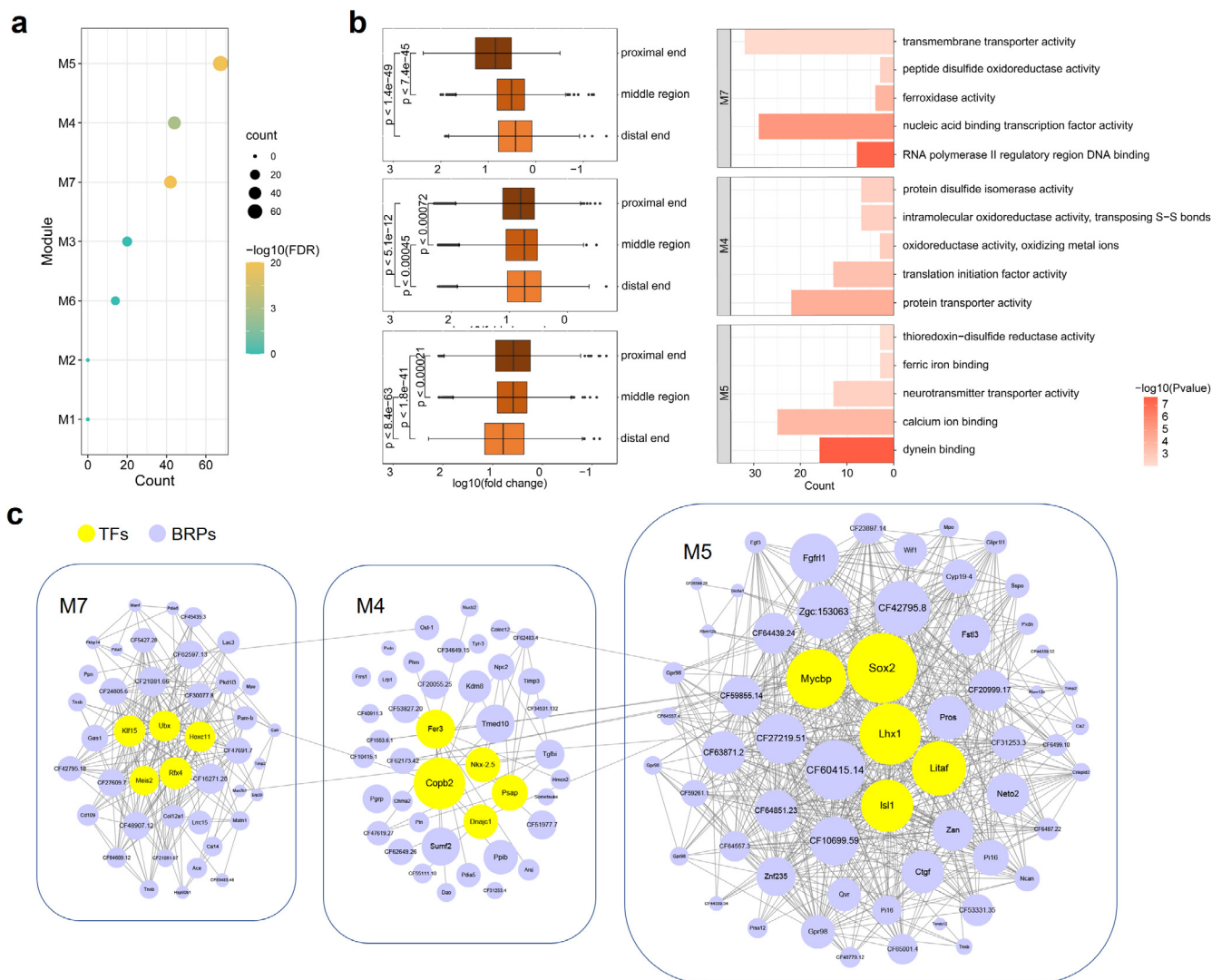


Fig. 4. Gene co-expression BRPs during byssal secretion. (a) The dot plot shows the distribution of BRPs across the module. The dot color represents the $-\log(\text{FDR})$ and the dot size indicates the count of BRPs (Table S7). (b) Gene expression patterns of different regions of foot during byssal secretion (left) and GO enrichment analysis of BRPs-enriched modules (right). Significantly enriched pathways with p -values < 0.01 reveal the functional roles of module genes (see Table S8 for the full result). The relative expression level was represented by the fold change of average TPMs at t1-t4 divided by t0 TPMs. (c) Gene co-expression network of scallop BRPs and hub TFs in M7, M4 and M5. The blue nodes represent candidate BRPs and the yellow nodes represent TFs. (For interpretation of the references to color in this figure legend, the reader is referred to the web version of this article.)

trate the dynamic process of byssal adhesion at molecular level. The classical foot-byssal complex proposed by Gruffydd et al. [16,71] hypothesized that the byssus ribbons were secreted by the primary byssus gland at the proximal end of foot, passing down along the byssus duct and eventually firmly attached to the substratum (Fig. 5a). However, according to the spatiotemporal expression patterns of scallop BRPs, we proposed that the secondary byssal gland running along the pedal groove was also involved in the secretion of byssus ribbons (Fig. 5b), which was thought to be merely responsible for the secretion of byssal sheaths [16,71]. There are three main points supporting our inference. First, as the main components of scallop byssus, the EGF-like domain containing proteins expressed at distinct foot regions and displayed an interesting spacial-related expression tendency, which was difficult to be explained by Gruffydd's model if the byssus ribbons were elongated from the proximal end. Secondly, most BRPs were simultaneously up-regulated at the initial stage t1 in three different foot regions during byssal secretion, which suggested the secretion of byssal proteins was not likely to be a

sequentially activated process extension. The participation of both the primary and secondary byssus gland could preferably explain the simultaneous expression pattern of scallop BRPs and meets the need of the rapid secretion of large amounts of byssus. Thirdly, the spatial expression patterns of the structural BRPs could better correspond to the components of each byssal region (byssal root, thread and plaque). For instance, the spatial expression tendency of EGF-like domain containing BRPs was consistent with the ultrastructural transformation from scallop byssal root (wavy coiled fibrils) to the thread (densely packed fibrils) [71]. Among them, CF52787.5 was specifically expressed in proximal end of foot and was proved to be indispensable for the integrity of scallop byssal root [19]. Moreover, the Tyr-rich BRP, CF53671.1, was highly expressed in the distal end and middle region of foot and likely to be involved in the formation of byssal cuticle, according to its high similarity with the cuticle protein Mefp1 in mussel [72]. Overall, different with the previous view that the byssal ribbon was produced by the primary byssus gland, our study proposed a new model of byssal secretion (Fig. 5a, b).

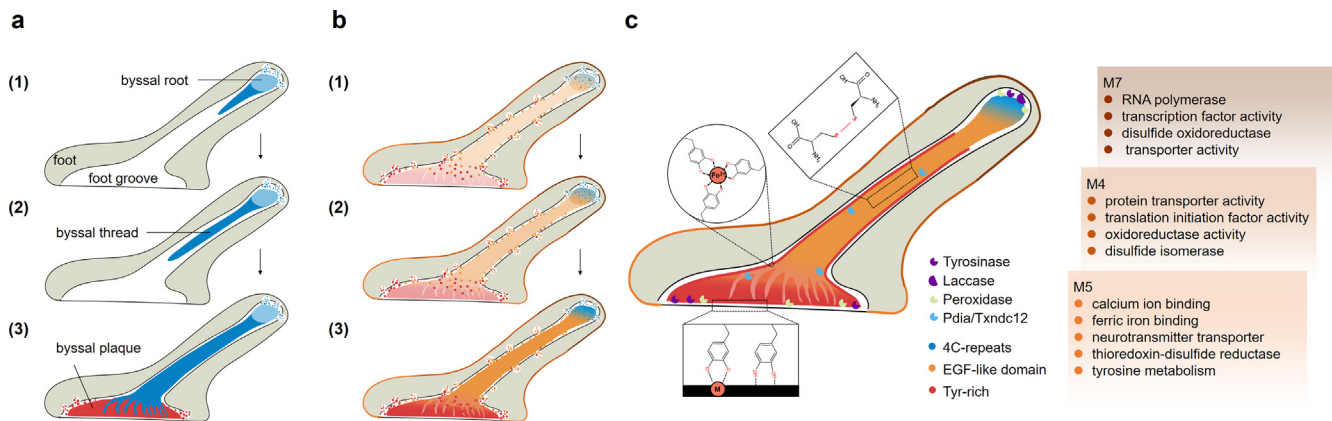


Fig. 5. Model of scallop byssal secretion and adhesion. (a) The “root-initiated secretion and extension-based assembly” model hypothesized by Gruffydd [16,71]: (1) The byssus ribbons produced by the primary byssus gland in proximal end of foot; (2) The byssal “raw materials” were stored in the byssus duct, it would be assembled and passed down along the byssus duct until required; (3) The byssus ribbons were eventually attached to the substratum by the distal end of foot and the byssal plaque formed. (b) The “foot-wide simultaneous secretion and in situ assembly” model of byssal secretion proposed by the present study: (1) Both the primary and secondary byssus glands (surrounding pedal groove) involved in the quick production of byssal ribbons; (2) The byssal “raw materials” were stored nearby until needed; (3) With the catalysis of enzymes and cross-linking between adhesive proteins, the “raw materials” were assembled quickly and a new byssus formed. (c) Hypothetical model of scallop byssal adhesion. The EGF-like domain containing, 4C-repeats containing and Tyr-rich BRPs are basic components of scallop byssus. Phenoloxidases, peroxidases and protein disulfide-isomerases dominate the modification and self-assembly of scallop byssal proteins. Key regulatory pathways (e.g., protein synthesis, disulfide bond oxidation and reduction, metal ion binding) participate in the byssal secretion and adhesion. Different foot regions were marked by the outer contour lines with different colors.

Byssal adhesion is a complex biological process, involving multi-level factors such as protein structure, post-translational modification and chelation of metal ion [73]. Benefiting from our comprehensive secretome profiling strategy, the main components of scallop byssus, the major enzymes and the key regulatory modules of byssal secretion and adhesion were identified (Fig. 5c). We revealed that the EGF-like domain containing BRPs were main components of scallop byssus, which were characterized by the “EC protein” chimeric structures (e.g., the EGFL/CBD fusion domain architecture). This characteristic was unique to scallop and our previous research regarded “EC protein” as a novel chimeric gene family resulted from a gene fusion event [19]. This structural evolutionary innovation probably enhances Ca^{2+} binding and strengthens the self-assembly properties of byssal proteins [74–76]. Gene translation, protein processing and protein transport processes were up-regulated and correlated well with the assembly and modification of scallop byssus during secretion process [16,71]. In the proximal end of foot, the 4C-repeats containing BRPs displayed the highest expression levels. Consistent with the 6-Cys residues in EGF-like domain, the 4C-repeats may also participate in the formation of intramolecular disulfide bonds, mediating the interactions with other byssal proteins [66]. In addition, vWFA domain containing BRPs were also up-regulated in the proximal end of foot during byssus secretion. The vWFA domain of scallop BRPs showed high sequence similarity with the mussel PTMP1 protein and ciona ASP1, which could contribute to the cross-linking between adhesive proteins [37,77]. The involvement of O-linked glycosylation and phosphorylation may contribute to protein stability and enhance cohesion and adhesion abilities [5,79,79]. Different from the collagenous thread of mussel, almost no collagen was detected in scallop byssus [71]. Although all three collagens identified in this study were up-regulated in the proximal end of foot, their expression levels were negligible, which suggested that collagens might act as “additives” contributing to the elasticity of byssal root [19]. In the distal end of foot, Tyr-rich BRPs were significantly activated during byssal secretion, which was involved in the formation of byssal thread and plaque. Based on the high sequence similarity with mussel Mefp1, CF53671.1 may be able to bind environmental Fe^{3+} ions to form a protective cuticle consisting of tris-dopa-iron coordination complexes, which could protect byssus against corrosion by seawater and degradation by

microorganisms[80]. Two other Tyr-rich BRPs (CF57509.5 and CF20079.1) with smaller molecular weight were supposed to be easy to diffuse and form more binding sites in the byssal plaque [81]. The metal ion binding, peroxidase activity and tyrosine metabolism related biological processes were significantly activated in distal end of scallop foot. These processes were known to play important roles in interfacial adhesion by forming strong cross-link between adhesive proteins [19,42,76,83,83] or in the oxidation of amino acid residues [9,85,85]. Our results suggested that these processes might contribute to the integrity of scallop byssal plaque.

Moreover, tyrosinase, laccase, peroxidase and enzymes involved in disulfide-bond formation dominant the modification of byssal adhesives, which were primary contributors to the rapid byssus assembly and adhesion. Tyrosinase is the key polyphenol oxidase that catalyzes the modification of tyrosine residues into DOPA. DOPA mediated the strong interface adhesion between byssal plaque and the underwater substrates by forming hydrogen bonds [8,9,85]. However, in the proximal end of foot, DOPA was oxidized into less adhesive DOPA-quinone by polyphenol oxidase laccase [8], which might enable the detach of scallop byssal root. The cross-linking pathway catalyzed by peroxidase was important to interfacial adhesion of barnacle cement [22,84]. Isomerase has been reported to catalyze the formation and breakage of disulfide bonds of EGF-like domain containing BRPs and contribute to the stability of the protein complex [28,86]. In addition, gene co-expression networks revealed the key transcription factors involved in the regulation of byssus secretion. Some neural stem cell marker genes, such as *Sox2* [87] and *Lhx1* [88], were hub genes in M5 module, while the genes associated with the neurotransmitter transporter activity were significantly up-regulated at the distal end of foot during the byssal secretion, which corresponded well with the perceptive function of foot to surrounding environment [16]. More interestingly, it has been reported that transcription factors *Sox2*, *Copb2*, *Meis2* and homeobox genes (*Lhx1*, *Ubx*, *Hoxc11*) were key regulators of hair follicle development [89–92], indicating the signs of convergence evolution between byssus secretion and hair growth. In contrast to the previously proposed “root-initiated secretion and extension-based assembly” model [16,71] that assumed the byssus ribbons were secreted by the primary byssus gland and assembled at the proximal end of foot, our

“foot-wide simultaneous secretion and in situ assembly” model hypothesized that both the primary and secondary byssus glands were involved in the rapid production of byssal ribbon, with the byssal “raw materials” of different regions of scallop byssus were secreted in situ by the byssus glands in the corresponding foot regions and stored in the nearby pedal groove until needed. When adhesion occurred, the “raw materials” quickly assembled in situ and a new byssus formed (Fig. 5). Our findings suggested the EGF-like domain containing proteins, the Tyr-rich proteins and 4C-repeats containing proteins were the main components of scallop byssus and the modification enzymes (e.g., peroxidase, tyrosinase, isomerase and laccase) primarily contributed to the rapid byssus assembly and adhesion. Prior to the attachment, the byssal “raw materials” would be assembled quickly with the catalysis of enzymes and cross-linking between adhesive proteins.

5. Conclusion

In this study, we proposed a computational pipeline for systematic profiling of byssus secretome based on the spatiotemporal transcriptomes of the scallop *C. farrari* and comprehensive characterization of gene features of scallop BRPs. A total of 186 BRPs were identified and categorized into three groups according to the sequence compositions and functional annotations. Our findings suggested the prevalence of adhesion-relevant protein features in putative structural BRPs and the related enzymes and proteinase inhibitors primarily responsible for the rapid byssus assembly and adhesion. Spatiotemporal expression and co-expression network analyses of BRPs revealed diverse functions on byssus secretion, which supported a novel “foot-wide simultaneous secretion and in situ assembly” model of scallop byssus secretion and adhesion. Overall, the byssal secretome-based approach provided important molecular resources for better understanding of the mechanisms behind byssal secretion and adhesion and established a common framework for other secretome profiling studies.

Declaration of Competing Interest

The authors declare that they have no known competing financial interests or personal relationships that could have appeared to influence the work reported in this paper.

Acknowledgements

We acknowledge the grant support from the Marine S&T Fund of Shandong Province for Pilot National Laboratory for Marine Science and Technology (Qingdao) (No.2022QNL050101-1), National Natural Science Foundation of China (32130107, 31900369), Key R&D Project of Shandong Province (2020ZLYS10), China Agriculture Research System of MOF and MARA, and Taishan Scholar Project Fund of Shandong Province of China.

Authors' contributions

S.W. and J.W. designed the project. X.D., X.Z., L.B., X.C., Y.M. and Yp.L. performed the analysis. J.W., L.B., X.D. and S.W. wrote the manuscript. Y.L., J.L., L.Z. and X.H. participated in discussions and provided suggestions for manuscript improvement. S.W. and Z.B. supervised the whole study. All authors read and approved the final manuscript.

Appendix A. Supplementary data

Supplementary data to this article can be found online at <https://doi.org/10.1016/j.csbj.2022.05.048>.

References

- [1] Xia J, Minamino S, Kuwabara K, Arai S. Stem cell secretome as a new booster for regenerative medicine. *Biosci Trends* 2019;13:299–307.
- [2] Xue H, Lu B, Lai M. The cancer secretome: A reservoir of biomarkers. *J Transl Med* 2008;6:52.
- [3] López de Andrés J, Griñán-Lisón C, Jiménez G, Marchal JA. Cancer stem cell secretome in the tumor microenvironment: A key point for an effective personalized cancer treatment. *J Hematol Oncol* 2020;13:136.
- [4] Luque M, Sanz-Alvarez M, Santamaría A, Zazo S, Cristóbal I, et al. Targeted therapy modulates the secretome of cancer-associated fibroblasts to induce resistance in *her2*-positive breast cancer. *Int J Mol Sci* 2021;22:13297.
- [5] Hennebert E, Maldonado B, Ladurner P, Flammang P, Santos R (2015) Experimental strategies for the identification and characterization of adhesive proteins in animals: A review. *Interface focus* 5: 20140064–20140064.
- [6] Almeida M, Reis RL, Silva TH. Marine invertebrates are a source of bioadhesives with biomimetic interest. *Mater Sci Eng: C* 2020;108:110467.
- [7] Priemel T, Palia G, Förste F, Jehle F, Sviben S, et al. Microfluidic-like fabrication of metal ion-cured bioadhesives by mussels. *Science* 2021;374:206–11.
- [8] Li X, Li S, Huang X, Chen Y, Cheng J, et al. Protein-mediated bioadhesion in marine organisms: A review. *Mar Environ Res* 2021;170:105409.
- [9] Stewart RJ. Protein-based underwater adhesives and the prospects for their biotechnological production. *Appl Microbiol Biotechnol* 2011;89:27–33.
- [10] Ou Q, Shu D, Zhang Z, Han J, Iten H, et al. The dawn of complex animal food webs: A new predatory anthozoan (Cnidaria) from the Cambrian of China. *The Innovation* 2021;3:100195.
- [11] Flammang P, Demeuldre M, Hennebert E, Santos R. Adhesive secretions in Echinoderms: A review. In: Smith AM, editor. *Biological Adhesives*. Cham: Springer International Publishing; 2016. p. 193–222.
- [12] Alejandrino A, Puslednik L, Serb J. Convergent and parallel evolution in life habit of the scallops (Bivalvia: Pectinidae). *BMC Evol Biol* 2011;11:164.
- [13] Liang C, Strickland J, Ye Z, Wu W, Hu B. Biochemistry of barnacle adhesion: An updated review. *Front Mar Sci* 2019;6:565.
- [14] Pennati R, Rothbacher U. Bioadhesion in ascidians: A developmental and functional genomics perspective. *Interface focus* 2015;5:20140061.
- [15] Shumway S. *Scallops: Biology, ecology and aquaculture*. Amsterdam: Elsevier; 1991. p. 1099.
- [16] Gruffydd L. The byssus and byssus glands in *Chlamys islandica* and other scallops (Lamellibranchia). *Zool Scr* 1978;7:277–85.
- [17] Li Y, Sun X, Hu X, Xun X, Zhang J, et al. Scallop genome reveals molecular adaptations to semi-sessile life and neurotoxins. *Nat Commun* 2017;8:1721.
- [18] Okutani T. *Marine mollusks in Japan*. Tokai University Press; 2000. p. 899.
- [19] Xu P, Dai X, Wang D, Miao Y, Zhang X, et al. The discovered chimeric protein plays the cohesive role to maintain scallop byssal root structural integrity. *Sci Rep* 2018;8:17082.
- [20] Zhang X, Dai X, Wang L, Miao Y, Xu P, et al. Characterization of an atypical metalloproteinase inhibitors like protein (Sbp8-1) from scallop byssus. *Front Physiol* 2018;9:597.
- [21] Zhang L, Sun Y, Jiao W, Li Y, Sun J, et al. Integration of transcriptomic and proteomic approaches provides a core set of genes for understanding of scallop attachment. *Mar Biotechnol* 2015;17:523–32.
- [22] Kamino K, Inoue K, Maruyama T, Takamatsu N, Harayama S, et al. Barnacle cement proteins: Importance of disulfide bonds in their insolubility. *J Biol Chem* 2000;275:27360–5.
- [23] Jonker J-L, Abram F, Pires E, Coelho A, Grunwald I, et al. Adhesive proteins of stalked and acorn barnacles display homology with low sequence similarities. *PLoS ONE* 2014;9:e108902.
- [24] Haemers S, Koper G, Frens G. Effect of oxidation rate on cross-linking of mussel adhesive proteins. *Biomacromolecules* 2003;4:632–40.
- [25] Yan G, Sun J, Wang Z, Qian P-Y, He L. Insights into the synthesis, secretion and curing of barnacle cyprid adhesive via transcriptomic and proteomic analyses of the cement gland. *Mar Drugs* 2020;18:186.
- [26] Davey PA, Power AM, Santos R, Bertemes P, Ladurner P, et al. Omics-based molecular analyses of adhesion by aquatic invertebrates. *Biol Rev Camb Philos Soc* 2021;96:1051–75.
- [27] Buffet J-P, Corre E, Duvernois-Berthet E, Fournier J, Lopez PJ. Adhesive gland transcriptomics uncovers a diversity of genes involved in glue formation in marine tube-building polychaetes. *Acta Biomater* 2018;72:316–28.
- [28] Santos R, Barreto Á, Franco C, Coelho AV. Mapping sea urchins tube feet proteome - A unique hydraulic mechano-sensory adhesive organ. *J Proteom Bioinform* 2013;79:100–13.
- [29] Liu F, Li Y, Yu H, Zhang L, Hu J, et al. MolluscDB: an integrated functional and evolutionary genomics database for the hyper-diverse animal phylum Mollusca. *Nucleic Acids Res* 2021;49:D988–97.
- [30] Dobin A, Davis CA, Schlesinger F, Drenkow J, Zaleski C, et al. STAR: Ultrafast universal RNA-seq aligner. *Bioinformatics* 2013;29:15–21.
- [31] Liao Y, Smyth GK, Shi W. featureCounts: An efficient general purpose program for assigning sequence reads to genomic features. *Bioinformatics* 2014;30:923–30.
- [32] Kassambara A, Mundt F (2020) Factoextra: Extract and visualize the results of multivariate data analyses. <https://CRAN.R-project.org/package=factoextra>.
- [33] Coyne K, Qin X-X, Waite J. Extensible collagen in mussel byssus: A natural block copolymer. *Science* 1997;277:1830–2.
- [34] Demartini D, Errico J, Sjöström S, Fenster A, Waite J. A cohort of new adhesive proteins identified from transcriptomic analysis of mussel foot glands. *J R Soc Interface* 2017;14:20170151.

- [35] Kang V, Lengerer B, Ruddy W, Flammang P. Molecular insights into the powerful mucus-based adhesion of limpets (*Patella vulgata* L.). *Open Biol* 2020;10:200019.
- [36] Lebesgue N, da Costa G, Ribeiro RM, Ribeiro-Silva C, Martins GG, et al. Deciphering the molecular mechanisms underlying sea urchin reversible adhesion: A quantitative proteomics approach. *J Proteomics* 2016;138:61–71.
- [37] Li S, Huang X, Chen Y, Li X, Zhan A. Identification and characterization of proteins involved in stolon adhesion in the highly invasive fouling ascidian *Ciona robusta*. *Biochem Biophys Res Commun* 2019;510(1):91–6.
- [38] Miao Y, Zhang L, Sun Y, Jiao W, Li Y, et al. Integration of transcriptomic and proteomic approaches provides a core set of genes for understanding of scallop attachment. *Mar Biotechnol* 2015;17(5):523–32.
- [39] Pjeta R, Lindner H, Kremser L, Salvenmoser W, Sobral D, et al. Integrative transcriptome and proteome analysis of the tube foot and adhesive secretions of the sea urchin *Paracentrotus lividus*. *Int J Mol Sci* 2020;21(3):946.
- [40] Pjeta R, Wunderer J, Bertermes P, Hofer T, Salvenmoser W, et al. (2019) Temporary adhesion of the proseriate flatworm *Minona ileanae*. *Philos Trans R Soc Lond, B, Biol Sci* 374(1784): 20190194–20190194.
- [41] Rodrigues M, Ostermann T, Kremser L, Lindner H, Beisel C, et al. Profiling of adhesive-related genes in the freshwater cnidarian *Hydra magnipapillata* by transcriptomics and proteomics. *Biofouling* 2016;32(9):1115–29.
- [42] Waite JH. Mussel adhesion - essential footwork. *J Exp Biol* 2017;220:517–30.
- [43] Wong T, Ozaki N, Zhang W-P, Sun J, Yoshimura E, et al. (2018) Identification of barnacle shell proteins by transcriptome and proteomic approaches: From molecular and nano-structural analyses to environmental science. In: *Biomaterialization*. pp. 105–112.
- [44] Zhao H, Robertson N, Jewhurst S, Waite J. Probing the adhesive footprints of *Mytilus californianus* byssus. *J Biol Chem* 2006;281:11090–6.
- [45] Sayers EW, Bolton EE, Brister JR, Canese K, Chan J, et al. Database resources of the national center for biotechnology information. *Nucleic Acids Res* 2022;50:D20–6.
- [46] The UniProt Consortium. UniProt: the universal protein knowledgebase in 2021. *Nucleic Acids Res* 2021;49:D480–9.
- [47] Petersen TN, Brunak S, von Heijne G, Nielsen H. SignalP 4.0: Discriminating signal peptides from transmembrane regions. *Nat Methods* 2011;8:785–6.
- [48] Palade GE. Intracellular aspects of the process of protein synthesis. *Science* 1975;189:867.
- [49] Zambelli F, Mastropasqua F, Picardi E, D'Erchia AM, Pesole G, et al. REntropy: An entropy-based tool for the detection of significant variation of gene expression across multiple RNA-Seq experiments. *Nucleic Acids Res* 2018;46:e46.
- [50] Krogh A, Larsson B, von Heijne G, Sonnhammer ELL. Predicting transmembrane protein topology with a hidden markov model: Application to complete genomes. *J Mol Biol* 2001;305:567–80.
- [51] Bagos P, Liakopoulos T, Hamodrakas S. Finding beta-barrel outer membrane proteins with a Markov Chain Model. *WSEAS Transac Biol Biomed* 2004;2:186–9.
- [52] Emanuelsson O, Brunak S, von Heijne G, Nielsen H. Locating proteins in the cell using TargetP, SignalP and related tools. *Nat Protoc* 2007;2:953–71.
- [53] Stothard P. The sequence manipulation suite: Javascript programs for analyzing and formatting protein and DNA sequences. *Biotechniques* 2000;28:1102–4.
- [54] Kyte J, Doolittle RF. A simple method for displaying the hydropathic character of a protein. *J Mol Biol* 1982;157:105–32.
- [55] Marchler-Bauer A, Lu S, Anderson JB, Chitsaz F, Derbyshire MK, et al. CDD: A conserved domain database for the functional annotation of proteins. *Nucleic Acids Res* 2011;39:D225–9.
- [56] Liu C. Comparative proteomics for an in-depth understanding of bioadhesion mechanisms and evolution across metazoans. *J Proteomics* 2022;256:104506.
- [57] Tamara K, Stecher G, Peterson D, Filipinski A, Kumar S. MEGA6: Molecular evolutionary genetics analysis version 6.0. *Mol Biol Evol* 2013;30:2725–9.
- [58] Gouet P, Robert X, Courcelle E. ESPript/ENDscript: Extracting and rendering sequence and 3D information from atomic structures of proteins. *Nucleic Acids Res* 2003;31:3320–3.
- [59] Wang D, Liu D, Yuchi J, He F, Jiang Y, et al. MusiteDeep: A deep-learning based webserver for protein post-translational modification site prediction and visualization. *Nucleic Acids Res* 2020;48:W140–6.
- [60] Wang J, Zhang L, Lian S, Qin Z, Zhu X, et al. Evolutionary transcriptomics of metazoan biphasic life cycle supports a single intercalation origin of metazoan larvae. *Nat Ecol Evol* 2020;4:725–36.
- [61] Langfelder P, Horvath S. WGCNA: An R package for weighted correlation network analysis. *BMC Bioinform* 2008;9:559.
- [62] Benjamini Y, Hochberg Y. Controlling the false discovery rate - A practical and powerful approach to multiple testing. *J Royal Statist Soc* 1995;57:289–300.
- [63] Chen S, Yang P, Jiang F, Wei Y, Ma Z, et al. De novo analysis of transcriptome dynamics in the migratory locust during the development of phase traits. *PLoS ONE* 2010;5:e15633.
- [64] Shannon P, Markiel A, Ozier O, Baliga NS, Wang JT, et al. Cytoscape: A software environment for integrated models of biomolecular interaction networks. *Genome Res* 2003;13:2498–504.
- [65] Zhang L, Zhang X, Wang Y, Xu P, Diao Z, et al. Identification and characterization of protein phosphorylation in the soluble protein fraction of scallop (*Chlamys farreri*) byssus. *Mol Biol Rep* 2019;46:4943–51.
- [66] Schrijver I, Liu W, Brenn T, Furthmayr H, Francke U. Cysteine substitutions in epidermal growth factor-like domains of fibrillin-1: Distinct effects on biochemical and clinical phenotypes. *Am J Hum Genet* 1999;65:1007–20.
- [67] Kang J, Stevenson A, Yau P, Kollmar R. *Sparc* protein is required for normal growth of zebrafish otoliths. *Assoc Res Otolaryngol* 2008;9:436–51.
- [68] Takahata Y, Hagino H, Kimura A, Urushizaki M, Kobayashi S, et al. *Smc1* and *Smc2* regulate bone formation as downstream molecules of *Runx2*. *Commun Biol* 2021;4:1199.
- [69] Santos C, Sonoda G, Cortez T, Coutinho L, Andrade S. Transcriptome expression of biomineralization genes in *Littoraria flava* gastropod in Brazilian rocky shore reveals evidence of local adaptation. *Genome Biol Evol* 2021;13.
- [70] Inoue K, Yoshioka Y, Tanaka H, Kinjo A, Sassa M, et al. Genomics and Transcriptomics of the green mussel explain the durability of its byssus. *Sci Rep* 2021;11:5992.
- [71] Gruffydd L, Budiman A, Nott J. The ultrastructure of the byssus and the byssus glands in *Chlamys varia* L. (Lamellibranchia). *J Mar Biol Assoc U K* 1979;59:597–603.
- [72] Kamino K. Underwater adhesive of marine organisms as the vital link between biological science and material science. *Mar Biotechnol* 2008;10:111–21.
- [73] Li S, Xia Z, Chen Y, Gao Y, Zhan A (2018) Byssus structure and protein composition in the highly invasive fouling mussel *Limnoperna fortunei*. *Front Physiol* 9: 418–418.
- [74] Hilge M, Aelen J, Vuister GW. Ca²⁺ regulation in the Na⁺/Ca²⁺ exchanger involves two markedly different Ca²⁺ sensors. *Mol Cell* 2006;22:15–25.
- [75] Alonso-García N, Inglés-Prieto A, Sonnenberg A, Pereda J. Structure of the Calx-beta domain of the integrin beta4 subunit: Insights into function and cation-independent stability. *Acta Crystallogr D Biol Crystallogr* 2009;65:858–71.
- [76] Hwang DS, Zeng H, Masic A, Harrington MJ, Israelachvili JN, et al. Protein- and metal-dependent interactions of a prominent protein in mussel adhesive plaques. *Biol Chem* 2010;285:25850–8.
- [77] Suhre MH, Gertz M, Steegborn C, Scheibel T. Structural and functional features of a collagen-binding matrix protein from the mussel byssus. *Nat Commun* 2014;5:3392.
- [78] Sun C, Fantner GE, Adams J, Hansma PK, Waite JH. The role of calcium and magnesium in the concrete tubes of the sandcastle worm. *J Exp Biol* 2007;210:1481–8.
- [79] Zhao H, Waite J. Linking adhesive and structural proteins in the attachment plaque of *Mytilus californianus*. *J Biol Chem* 2006;281:26150–8.
- [80] Harrington M, Masic A, Holten-Andersen N, Waite J, Fratzl P. Iron-Clad Fibers: A metal-based biological strategy for hard flexible coatings. *Science* 2010;328:216–20.
- [81] Lin Q, Gourdon D, Sun C, Holten-Andersen N, Anderson T, et al. Adhesion mechanisms of the mussel foot proteins mfp-1 and mfp-3. *Proc Natl Acad Sci* 2007;104:3782–6.
- [82] Holten-Andersen N, Toprak M, Stucky G, Zok F, Waite J. Metals and the integrity of a biological coating: The cuticle of mussel byssus. *Langmuir* 2009;25:3323–6.
- [83] Hennebert E, Wattiez R, Demeuldre M, Ladurner P, Hwang DS, et al. Sea star tenacity mediated by a protein that fragments, then aggregates. *Proc Natl Acad Sci* 2014;111:6317.
- [84] So CR, Scancella JM, Fears KP, Essock-Burns T, Haynes SE, et al. Oxidase activity of the barnacle adhesive interface involves peroxide-dependent catechol oxidase and lysyl oxidase enzymes. *ACS Appl Mater Interfaces* 2017;9:11493–505.
- [85] Lee B, Dalsin J, Messersmith P. Synthesis and gelation of DOPA-modified poly(ethylene glycol) hydrogels. *Biomacromolecules* 2002;3:1038–47.
- [86] Gao Y, Mehta K. Interchain disulfide bonds promote protein cross-linking during protein folding. *J Biochem* 2001;129:179–83.
- [87] Ellis P, Fagan B, Magness S, Hutton S, Taranova O, et al. *Sox2*, a persistent marker for multipotential neural stem cells derived from embryonic stem cells, the embryo or the adult. *Dev Neurosci* 2004;26:148–65.
- [88] Peretz Y, Kohl A, Slutsky N, Komlos M, Varshavsky S, et al. Neural stem cells deriving from chick embryonic hindbrain recapitulate hindbrain development in culture. *Sci Rep* 2018;8:13920.
- [89] Driskell R, Giangreco A, Jensen K, Mulder K, Watt F. *Sox2*-positive dermal papilla cells specify hair follicle type in mammalian epidermis. *Development* 2009;136:2815–23.
- [90] Pirastu N, Joshi P, de Vries P, Cornelis M, McKeigue P, et al. GWAS for male-pattern baldness identifies 71 susceptibility loci explaining 38% of the risk. *Nat Commun* 2017;8:1584.
- [91] Jave Suarez L, Schweizer J. The *Hoxc13*-controlled expression of early hair keratin genes in the human hair follicle does not involve *Tale* proteins *Meis* and *Prep* as cofactors. *Arch Dermatol Res* 2006;297:372–6.
- [92] Duverger O, Morasso M. Role of homeobox genes in the patterning, specification, and differentiation of ectodermal appendages in mammals. *J Cell Physiol* 2008;216:337–46.